

RESEARCH ARTICLE

SPECIAL ISSUE: CELL BIOLOGY OF THE IMMUNE SYSTEM

RHOA-mediated mechanical force generation through Dectin-1

Rohan P. Chorasge¹, Tomasz Kołodziej¹, Alan Buser¹, Zenon Rajfur² and Aaron K. Neumann^{1,*}

ABSTRACT

Dendritic cell-associated C-type lectin 1 (Dectin-1, also known as CLEC7A) is an innate immune pattern recognition receptor that recognizes β -glucan on the *Candida albicans* cell wall. Recognition of β -glucan by immune cells leads to phagocytosis, oxidative burst, cytokine and chemokine production. We looked for specific mechanisms that coordinate phagocytosis downstream of Dectin-1 leading to actin reorganization and internalization of fungus. We found that stimulation of Dectin-1 by soluble β -glucan leads to mechanical force generation and areal contraction in Dectin-1-transfected HEK-293 cells and M1 macrophages. With inhibitor studies, we found this force generation is a spleen tyrosine kinase (SYK)-independent, but SRC family kinase (SFK)-dependent process mediated through the RHOA–ROCK–myosin light chain (MLC) pathway. We confirmed activation of RHOA downstream of Dectin-1 using activity assays and stress fiber formation. Through phagocytosis assays, we found direct evidence for the importance of RHOA–ROCK–MLC signaling in the process of phagocytosis of *C. albicans*.

KEY WORDS: *Candida albicans*, Dectin-1, RHOA, Fungal pathogen, Mechanobiology

INTRODUCTION

Dendritic cell-associated C-type lectin 1 (Dectin-1, also known as CLEC7A) is a pattern recognition receptor expressed primarily on cells of myeloid origin, including macrophages, dendritic cells and neutrophils (Brown, 2006). The ligand for Dectin-1 is a highly immunogenic glucose polysaccharide with a backbone of β -(1,3)-linked linear units and β -(1,6)-linked side chains known as β -glucan (Goodridge et al., 2009). Glucans are ubiquitous in the fungal cell walls and form 50–60% of the dry weight of *Candida albicans* cell walls (Gow et al., 2012). Recognition of β -glucan by immune cells contributes to a variety of responses in these cells, including non-opsonic phagocytosis, oxidative burst, regulation of transcription, production of inflammatory cytokines and chemokines, and initiation of adaptive immunity (Plato et al., 2013). While Dectin-1 is expressed in up to eight different alternatively spliced isoforms, this paper will refer only to the predominant full-length A isoform (Willment et al., 2001). Dectin-1 signals via spleen tyrosine kinase (SYK)-dependent and SYK-independent pathways. Downstream signaling elements activated upon recognition of β -glucan by Dectin-1 include SRC family kinases (SFKs), SYK and caspase recruitment domain-containing protein 9 (CARD-9) to eventually mediate the production of reactive

oxygen species (ROS), activation of nuclear factor κ B (NF- κ B) and subsequent secretion of pro-inflammatory cytokines (Plato et al., 2013). Dectin-1 is known to signal via mechanisms that involve phosphorylation of its cytoplasmic tail by SFKs, leading to recruitment of SYK to the activated Dectin-1 cytoplasmic tail. SYK is then activated and phosphorylates downstream targets. Two major pathways are activated in a SYK-dependent manner: a pathway that leads to store-operated calcium release, nuclear factor of activated T-cells (NFAT) activation and a protein kinase C (PKC)-dependent pathway that leads to activation of a CARD9-dependent signaling complex, which results in NF- κ B activation (Plato et al., 2013; Goodridge et al., 2007; Sun and Zhao, 2007). The SYK-independent pathway requires activation of human RAS and RAF1, leading to activation of mitogen-activated protein kinases (MAPKs) (Gringhuis et al., 2009).

Phagocytosis is a mechanism by which a cell engulfs particles typically $>0.5\ \mu\text{m}$. In opsonic phagocytosis, a particle is coated by IgG and/or complement before being phagocytosed (Flannagan et al., 2012). Opsonic phagocytosis by these two opsonins involves different patterns of RHO family GTPase activation and actin reorganization to complete engulfment. Type I opsonic phagocytosis by Fc γ R involves pseudopod extension and ‘zippering’ of pseudopodial membrane extensions around the particle. In contrast, type II opsonic phagocytosis through binding of complement receptors, such as integrin $\alpha_M\beta_2$ (also known as CR3, Mac-1 and CD11b/CD18), to C3b and its proteolysis product invokes a phagocytic process characterized by ‘sinking’ of the particle into cell body without obvious pseudopod extension (Le Cabec et al., 2002). These rapid and dramatic changes in local cellular morphology require actin reorganization driven by RHO-family small GTPases. During type I phagocytosis, local pseudopod formation and membrane ruffling is thought to be mediated through RHO GTPases, such as RAC1 and CDC42. In contrast, sinking of particles in type II phagocytosis is thought to be mediated by contraction of actomyosin network in a RHOA-dependent manner (Le Cabec et al., 2002; Aderem and Underhill, 1999; Olazabal et al., 2002).

Cells of the innate immune system can also engulf particles through non-opsonic phagocytic processes, such as recognition of β -(1,3)-glucan on *Candida* species fungal pathogens by Dectin-1 (Brown et al., 2002; Herre et al., 2004). Additionally, direct interaction of integrin $\alpha_M\beta_2$, via its unique lectin-like domain, is also important for *Candida* uptake by human neutrophils (O’Brien et al., 2012), and signaling cross-talk between Dectin-1 and integrin $\alpha_M\beta_2$ has been described (Li et al., 2011). However, overall, Dectin-1-mediated phagocytosis is thought to be the major mechanism of non-opsonic recognition of glucan by macrophages and dendritic cells (Brown et al., 2002; Taylor et al., 2002).

Relative to opsonic phagocytic mechanisms, the specific signal transduction mechanisms leading to RHO-family GTPase activation and actin reorganization in Dectin-1-mediated phagocytosis have received less attention. Previous studies of Dectin-1-mediated phagocytosis of zymosan in murine macrophages have suggested

¹Department of Pathology, University of New Mexico, Albuquerque, NM 87131, USA. ²Institute of Physics, Jagiellonian University, Krakow 30-348, Poland.

*Author for correspondence (akneumann@salud.unm.edu)

© A.K.N., 0000-0002-1689-8324

that RAC2 and CDC42 are required, consistent with the activation of the guanine nucleotide exchange factor (GEF) VAV1 (Herre et al., 2004). Previous studies have also found that non-opsonic recognition through Dectin-1 is SYK independent (Herre et al., 2004; Goodridge et al., 2012). However, SYK is required for activation of the RHO-GEF VAV1 during glucan phagocytosis in microglia (Shah et al., 2009) and there is evidence for variable involvement of SYK in Dectin-1 mediated effector functions between various cell types (Herre et al., 2004; Rogers et al., 2005).

In this study, we present evidence that Dectin-1 activation by β -(1,3)-glucan causes SYK-independent activation of the small GTPase RHOA. The consequent actomyosin-dependent contraction of the cellular cortex leads to substantial mechanical force generation downstream of Dectin-1. Dectin-1- and RHOA-mediated generation of mechanical force through actomyosin network is important for non-opsonic engulfment of fungal particles (Yi et al., 2012; Goodridge et al., 2011).

RESULTS

Dectin-1-mediated glucan-dependent cellular contraction

We observed that Dectin-1-expressing HEK-293 cells undergo areal contraction within minutes after stimulation with medium molecular mass (MMW, ~150 kDa) glucan (Fig. 1A). This model provides an advantageous platform that can support Dectin-1 signaling and where Dectin-1 expression (and isoform distribution) can be strictly controlled. MMW glucan is thought to mimic some structural characteristics of glucans in the cell wall, including having a higher degree of triple-helical structure than seen in low molecular mass (LMW) glucans, such as laminarin. We found a statistically significant difference in the cell area between control and Dectin-1-expressing cells starting at ~180 s after stimulation with MMW glucan (Fig. 1B). To further test our hypothesis in a system chosen for greater physiological relevance, we performed similar experiments in M1 macrophages differentiated from human peripheral blood monocytes (Brown et al., 2002; Liu et al., 2015; Fischer et al., 2017). Areal contraction, similar to that observed with Dectin-1-expressing HEK-293 cells was also observed in M1 macrophages (Fig. 1C,D). These results suggest the biological relevance and possible existence of a glucan-sensitive mechanical force generation pathway downstream of Dectin-1 in human primary macrophages.

Cells generate and apply mechanical forces to their environment, typically in the pico- to nano-Newton range. Phagocytes exhibit an increase in cortical tension during the process of phagocytosis, exerting forces upon particles during their engulfment (Herant et al., 2006). One way to show and measure mechanical force application to the cellular microenvironment is traction force microscopy (TFM). With TFM, we can measure these forces as local shear stresses (i.e. traction forces exerted by a cell on their elastic substrate). We used TFM to measure the additional stresses exerted on the substrate by Dectin-1-expressing HEK-293 cells upon stimulation with MMW glucan. As HEK-293 cells undergo adhesion/migration-related cycles of contraction and relaxation, they exhibit basal fluctuations in traction forces. These pre-stimulation traction forces reached maximum amplitudes averaging 13.03 pN/ μm^2 (relative to the pre-stimulation phase mean traction force). After stimulation with MMW glucan, the mean traction forces increased to an extent that was considerably larger than could be accounted for by basal fluctuations in traction forces. The average increase in traction force post-stimulation (relative to the pre-stimulation phase mean traction force) was 22.75 pN/ μm^2 . A total of 25 independent traction force

measurements were conducted, of which $n=20$ were used to calculate traction forces. Five measurements were excluded due to technical concerns during data acquisition (detailed in Materials and Methods) that made traction force measurements from these datasets unreliable. Thus, we found a significant increase in mean traction after stimulation with glucan compared to pre-stimulation condition (Fig. 1E). These data confirm that substantial mechanical forces are generated downstream of Dectin-1 activation by fungal glucan. If the loss of cell body area observed in glucan-stimulated cells were merely due to de-adhesion, traction forces would have simply relaxed from the basal state upon loss of cell body area. The fact that we observed increased traction force concomitant to decreased cell body area is more consistent with a model wherein the observed loss of cell body area upon glucan stimulation is caused by cortical contraction of actomyosin networks downstream of Dectin-1.

While mechanical force generation is clearly important for any phagocytic process, a specific signaling mechanism driving Dectin-1-dependent contraction of cortical actomyosin networks has not been clearly delineated. We hypothesized that such a signaling mechanism must exist in order to explain the observed Dectin-1-mediated contractile phenomenon. Integrin activation has been associated with RHOA activation and actomyosin contraction. However, HEK-293 cells do not express the glucan-binding integrin $\alpha_M\beta_2$ (Cell atlas; <https://www.proteinatlas.org/ENSG00000169896-ITGAM/cell>). Furthermore, control HEK-293 cells not expressing Dectin-1 failed to exhibit contraction in response to glucan stimulation (Fig. 1B). Therefore, we assert that Dectin-1 does trigger a cellular mechanical force generation response, and we focused on understanding Dectin-1 signaling mechanisms required to initiate this response.

The biochemical signaling pathway downstream of Dectin-1 involved in force generation

We first tested the requirement for several membrane-proximal kinases in the areal contraction mediated by MMW glucan ligation of Dectin-1 (Fig. 2A). We found that the most membrane-proximal kinases in the Dectin-1 pathway, SFKs, were required for areal contraction after MMW glucan stimulation of Dectin-1-expressing cells. Treatment with PP1, which is a selective competitive inhibitor of ATP-binding of the SRC tyrosine kinase family (Tatton et al., 2003) also almost completely abolished the contractile response. Treatment with a broad-spectrum PKC inhibitor had no impact on the Dectin-1-mediated areal contractility response, demonstrating that the PKC/CARD9 arm of Dectin-1 signal transduction is dispensable for mechanical force generation. Additionally, CARD9 is very poorly expressed in HEK-293 cells, suggesting that this pathway is minimally operative, if at all, in this model (Cell atlas; <https://www.proteinatlas.org/ENSG00000187796-CARD9/cell>). Interestingly, BAY 61-3606, which potently inhibits SYK activity in an ATP-dependent manner, caused no significant decrease in Dectin-1-mediated cell contractility, suggesting that the membrane proximal signaling events leading to mechanical force generation downstream of Dectin-1 are SYK independent (Yamamoto, 2003). Because known SYK-independent signaling of Dectin-1 involves RAF-1 activation, which can lead to ERK1 and ERK2 (ERK1/2; also known as MAPK3 and MAPK1, respectively) MAPK activation, we inhibited the MAPKKs MEK1 and MEK2 (MEK1/2; also known as MAP2K1 and MAP2K2, respectively) that activate ERK1/2 MAPKs. Disruption of this SYK-independent MAPK signaling pathway had no significant impact on cellular areal contraction. We observed generally similar results in the human primary M1 macrophage model with all membrane-proximal kinase inhibitors (Fig. 2D). We

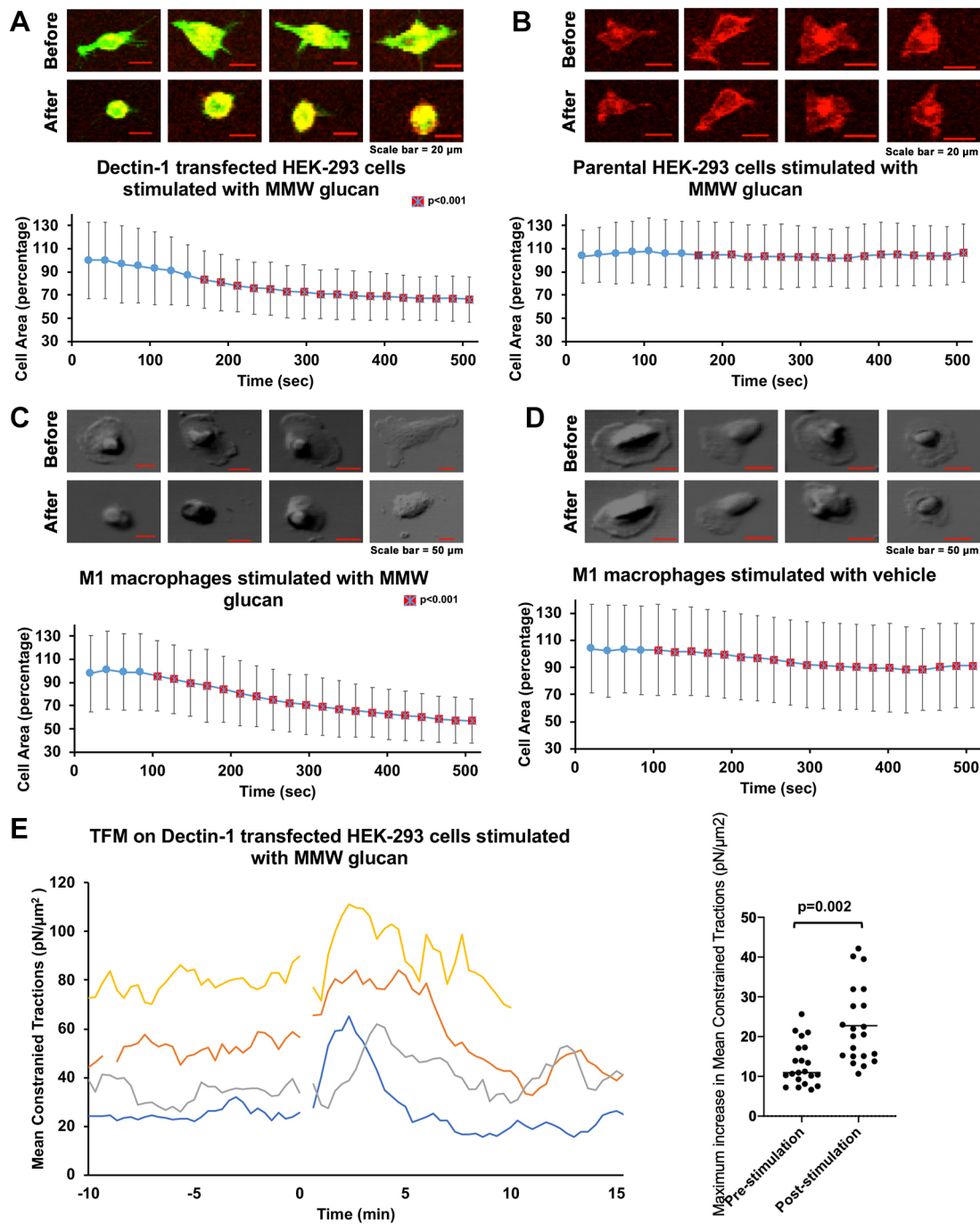


Fig. 1. Dectin-1-mediated glucan-dependent cellular contraction. (A) HEK-293 cells transfected with Emerald–Dectin-1 (green) and stained with Cell Mask Deep Red (CMDR). Images labeled ‘Before’ are pre-stimulation cells and those labeled ‘After’ are 500 s after stimulation with MMW glucan. Scale bars: 20 μ m. The area at each time point was normalized to the average cell area of Dectin-1 transfected HEK-293 cells observed prior to glucan stimulation and given as a percentage. MMW glucan was added at time 0. $n=29$ total cells pooled from ≥ 3 independent experimental replicates. (B) Control HEK-293 cells stained with CMDR, pre-stimulation and 500 s after stimulation with MMW glucan. Data were normalized as in A. Scale bars: 20 μ m. $n=31$ total cells pooled from ≥ 3 independent experimental replicates. (C) DIC images of M1 macrophages before and after stimulation with MMW glucan. Scale bars: 50 μ m. $n=31$ total cells pooled from ≥ 3 independent experimental replicates. Data were normalized as in A. (D) DIC images of mock-stimulated M1 macrophages. Scale bar: 50 μ m. $n=28$ total cells pooled from ≥ 3 independent experimental replicates. Data were normalized as in A. Data in A–D represent sample mean \pm s.d. Red squares with a cross indicate significant difference ($P < 0.01$) in cell area at a time point between the Dectin-1-transfected cells and control cells in B, or M1 macrophages (in C) compared with control macrophages (in D). (E) Mean constrained tractions from four independent HEK-293 cells transfected with Emerald–Dectin-1 illustrating increased traction force after stimulation with MMW glucan. Dot plot indicates the mean maximum increase in mean constrained tractions of individual cells with standard deviation, pre- and post-stimulation with glucan ($n=20$ independent cells).

conclude that mechanical force generation downstream of Dectin-1 requires a SFK-dependent process that does not appear to be mediated by any major known signaling mechanisms of Dectin-1.

Because no known Dectin-1 intracellular signaling pathways are clearly connected to cellular force generation mechanisms that could explain the observed contractile phenomenon, we proceeded

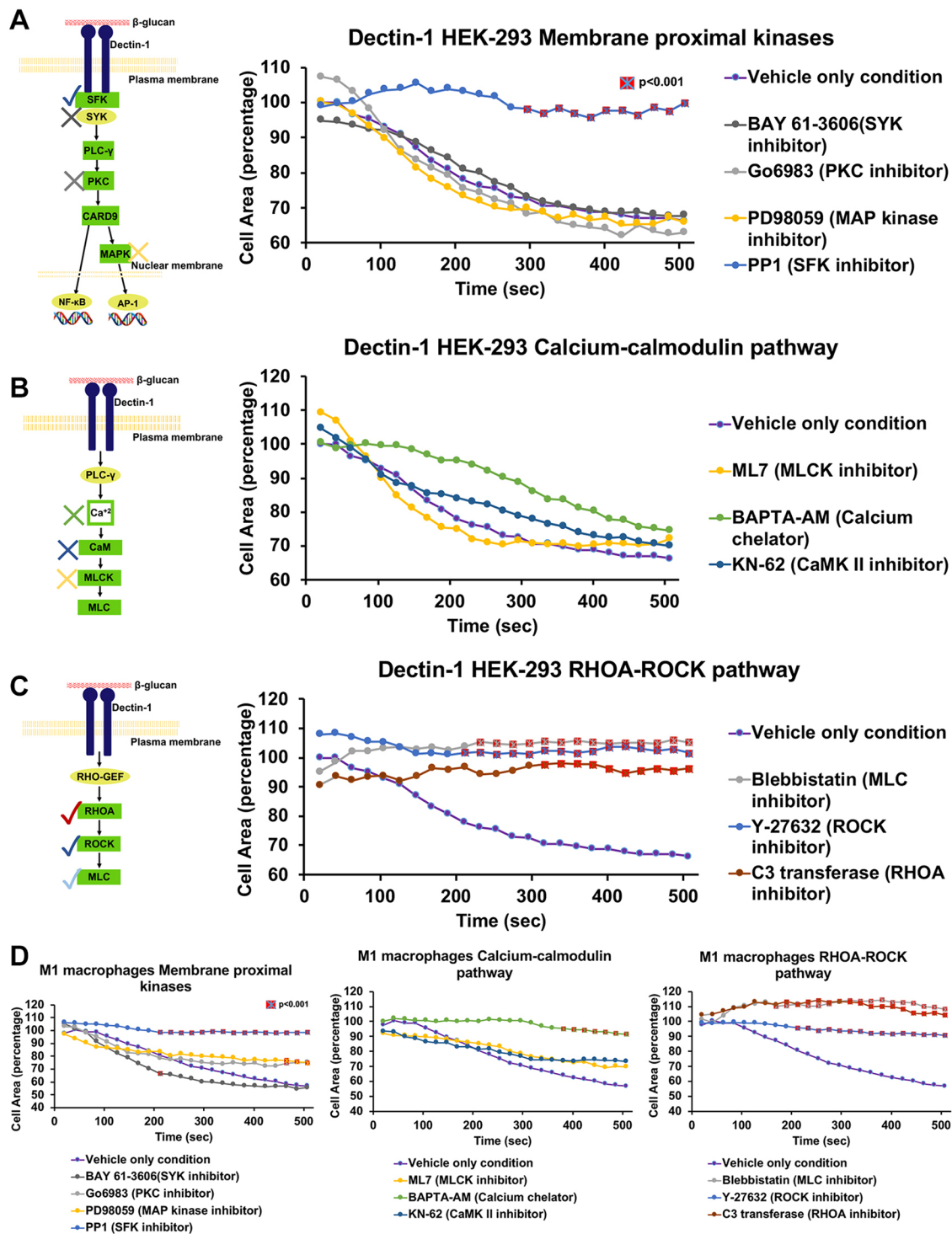


Fig. 2. Biochemical signaling pathway downstream of Dectin-1 involved in force generation. (A) HEK-293 cells transfected with Dectin-1 pretreated with BAY-61-3606 (SYK inhibitor) at 500 nM ($n=26$), Go6983 (PKC inhibitor) at 2 μ M ($n=24$), PD98059 (MAP kinase inhibitor) at 12.5 μ M ($n=26$) or PP1 (SRC inhibitor) at 10 μ M ($n=28$) for 1 h; stimulated with 8 μ g/ml MMW glucan and observed for change in area over 500 s. Each time point is normalized to the average HEK-293 cell area in the no inhibitor condition and given as a percentage. Only PP1 showed significant inhibition of contractility. (B) HEK-293 cells transfected with Dectin-1 pretreated with ML7 (MLCK inhibitor) at 25 μ M ($n=36$), BAPTA-AM (Ca^{2+} chelator) at 5 μ M ($n=23$) or KN-62 (Ca^{2+} /calmodulin-dependent kinase type II inhibitor) at 20 μ M ($n=23$) for 1 h; stimulated with 8 μ g/ml MMW glucan and observed for change in area over 500 s. None of these inhibitors were able to inhibit contractility significantly. (C) HEK-293 cells transfected with Dectin-1 pretreated with either Blebbistatin (myosin II inhibitor) at 12.5 μ M ($n=35$), Y-27632 (MLCK inhibitor) 5 μ M ($n=35$) for 1 h or C3 transferase (RHOA inhibitor) 1.5 μ g/ml ($n=25$) for 2 h; stimulated with 8 μ g/ml MMW glucan and observed for change in area over 500 s. All three inhibitors of this pathway showed significant inhibition of contractility. The diagrams on the left of A-C show currently well recognized pathways for cellular force generation. (D) M1 macrophages pretreated with BAY-61-3606 ($n=24$), Go6983 ($n=22$), PD98059 ($n=23$), PP1 ($n=24$), ML7 ($n=22$), BAPTA-AM ($n=23$), KN-62 ($n=20$), Blebbistatin ($n=21$), Y-27632 ($n=25$) for 1 h or C3 transferase ($n=23$) for 2 h; stimulated with 8 μ g/ml MMW glucan and observed for change in area over 500 s. Each time point is normalized to average macrophage cell area in the no inhibitor condition and given as a percentage. Red squares with a cross indicate significant difference ($P < 0.01$) in cell area at a time point between the inhibitor condition and vehicle only condition. All inhibitors showed similar results as HEK-293 cells except for BAPTA-AM, which showed inhibition of contractility at later time points. All values of 'n' denote a total number of cells pooled from ≥ 3 independent experimental replicates for the indicated experimental condition.

to broadly consider cellular mechanisms of mechanical force generation. Cellular force generation proceeds through two main effector mechanisms, both of which finally impinge on actin-myosin based contraction (Fukata et al., 2001). First, muscle cells generate force via a Ca^{2+} /calmodulin dependent process that leads to myosin light chain kinase (MLCK) activation, phosphorylation of myosin light chain (MLC) and activation of actomyosin contraction. Second, other cell types utilize a different pathway (e.g. for cell migration) that involves activation of RHOA, leading to ROCK (herein referring to ROCK1 and ROCK2) activation, phosphorylation of MLC and initiation of actomyosin contraction.

In smooth muscles, release of sarcoplasmic reticulum (SR) Ca^{2+} leads to formation of activation of CaM (calmodulin) signaling, which activates MLCK for phosphorylation of MLC to drive actomyosin contraction (Fukata et al., 2001). We found that KN-62, which is a selective, cell permeable inhibitor of Ca^{2+} /calmodulin-dependent kinase type II (CaMK II, the upstream Ca^{2+} -dependent activator of CaM), and ML-7, which is a muscle MLCK inhibitor, do not inhibit contractility downstream of Dectin-1 in the HEK-293 model (Fig. 2B) (Tokumitsu et al., 1990; Saitoh et al., 1987). We observed similar results in the human primary M1 macrophage model with KN-62 and ML-7 inhibitors (Fig. 2D). BAPTA-AM is a cell-permeable Ca^{2+} chelator that blocks Ca^{2+} /CaM activation by binding and inactivating cytoplasmic Ca^{2+} (Tang et al., 2007). Inhibition with BAPTA-AM does not block glucan-stimulated contractility mediated via Dectin-1 contractility in the HEK-293 cell model (Fig. 2B). BAPTA-AM inhibition does reach statistical significance for M1 macrophages at late time points (Fig. 2D). This BAPTA-AM result may point to a greater reliance on cytoplasmic Ca^{2+} in M1 macrophages, but we do recognize the pleiotropic effects of Ca^{2+} on cell biology, which complicates interpretation of BAPTA-AM results. Overall, we found that inhibition of the Ca^{2+} /calmodulin pathway using several inhibitors against distinct steps in this pathway uniformly showed no significant effect on the Dectin-1-mediated contractile response. This led us to conclude that a Ca^{2+} /calmodulin-dependent pathway is not involved in Dectin-1-mediated force generation.

Next, we tested inhibitors against RHOA and ROCK to determine the involvement of the second pathway (RHOA–ROCK–MLC). C3 transferase, which specifically inhibits RHOA through ADP-ribosylation on asparagine 41 in the effector binding domain of the GTPase (Wilde and Aktories, 2001), inhibited contractility in Dectin-1-transfected cells (Fig. 2C). Y-27632, which inhibits the kinase activity ROCK in a ATP-competitive manner (Fukata et al., 2001), also showed significant inhibition of contractility (Fig. 2C). Blebbistatin blocks phosphate dissociation from the myosin–ADP–phosphate complex, trapping myosin heads in the actin-detached state and leading to relaxation of actomyosin filaments (Kovács et al., 2004). We found that blebbistatin profoundly inhibits Dectin-1-mediated contractility (Fig. 2C). From these studies in the HEK-293 model, we concluded that the RHOA-based force generation pathway is engaged downstream of Dectin-1 activation by glucan, leading to myosin II activation and actomyosin contractility. Furthermore, we also confirmed that the RHOA–ROCK–MLC pathway drives contractility downstream of Dectin-1 in M1 macrophages, where we observed strong inhibition of glucan-induced contractility by C3 transferase, Y-27632 and blebbistatin (Fig. 2D). Taken together, these data strongly support a model of RHOA activation downstream of Dectin-1, leading to contraction of the membrane subjacent actomyosin networks that control the mechanical properties of the cell and its ability to generate mechanical force.

Activation of RHOA downstream of Dectin-1 after stimulation with glucan

Activation of small GTPases, such as RHOA, RAC1 and CDC42, gives rise to typical morphological responses, including formation of actin stress fibers, lamellipodial/pseudopodial extension and filopodial extension, respectively (Nobes and Hall, 1995). Dectin-1-transfected cells, on stimulation with glucan, predominately showed increased formation of actin stress fibers, a phenotype consistent with activation of RHOA (Fig. 3A). For this assay, we used LifeAct transfection to stain actin structures. For analysis, we used a method reported in Rogge et al. (2017), which segments and quantifies actin fluorescence that is present in linear structures (e.g. stress fibers). We compared actin fluorescence coming from linear structures to total actin fluorescence, pre- and post-stimulation with glucan. We found a significant increase in the proportion of fluorescence coming from linear structures to total actin fluorescence in the post-stimulation condition. To further support activation of RHOA, we used RHOA G-LISA, a small G-protein activation assay. This is an ELISA-like assay for small family GTPase activation. We observed an increase in active RHOA within minutes of Dectin-1 stimulation by G-LISA (Fig. 3B). We did not find significant change in CDC-42 and RAC-1 activity after stimulation with glucan. These observations confirm and support our conclusion that Dectin-1 stimulation by soluble MMW glucan reliably induces a contractile response of the cell body, and that this force-generative response depends upon SFKs, the small GTPase RHOA, ROCK and myosin II (Fig. 3C).

Relevance of force generation pathway in non-opsonic phagocytosis mediated by Dectin-1

Next, we examined the importance of mechanical force generation in non-opsonic phagocytosis downstream of Dectin-1. HEK-293 cells transfected with Dectin-1 were presented with a high glucan-exposure *C. albicans* clinical isolate strain, TRL035, stained with Calcofluor and Cypher5E, a dye which registers entry into the acidic phagolysosome via a substantial increase in fluorescence. Following 1 h of exposure to yeast in the presence or absence of inhibitors of the RHOA pathway, both the phagocytic index (Fig. 4A), a measure of the efficiency of phagocytosis for captured fungal particles, and phagocytic activity, the fraction of cells that phagocytosed yeast, were calculated. Inhibition of RHOA, ROCK or myosin II significantly decreased both measures of Dectin-1-dependent phagocytosis, confirming an important role for this contractility signaling pathway in Dectin-1-mediated phagocytosis. The phagocytosis index is indicative of the efficiency of the phagocytic machinery in individual cells to phagocytose fungus. Phagocytic activity is indicative of generalized effect of inhibitor on the ability of a cell to phagocytose at least a single fungus. Using the human M1 macrophage system, we performed similar phagocytosis assay with TRL035 *C. albicans* and demonstrated a significant decrease in Dectin-1-mediated phagocytosis upon treatment with RHOA inhibitor, ROCK inhibitor and myosin II inhibitor indicating the importance of the RHOA-based pathway for phagocytosis of fungi in macrophages (Fig. 4B).

We observed that, while Dectin-1-mediated phagocytosis is markedly reduced in cells subjected to inhibition of the ROCK/RHOA pathway, partial actin phagocytic cups were observed in 75% of contacts with yeast in RHOA-inhibited cells (Fig. 4C). This suggested the RHOA activity might be required for complete maturation of the phagocytic synapse, leading to closure of the cup, particle engulfment and formation of the phagolysosome.

RHOA-dependent phagocytosis typically involves sinking type II phagocytosis. To confirm such morphology of Dectin-1-dependent

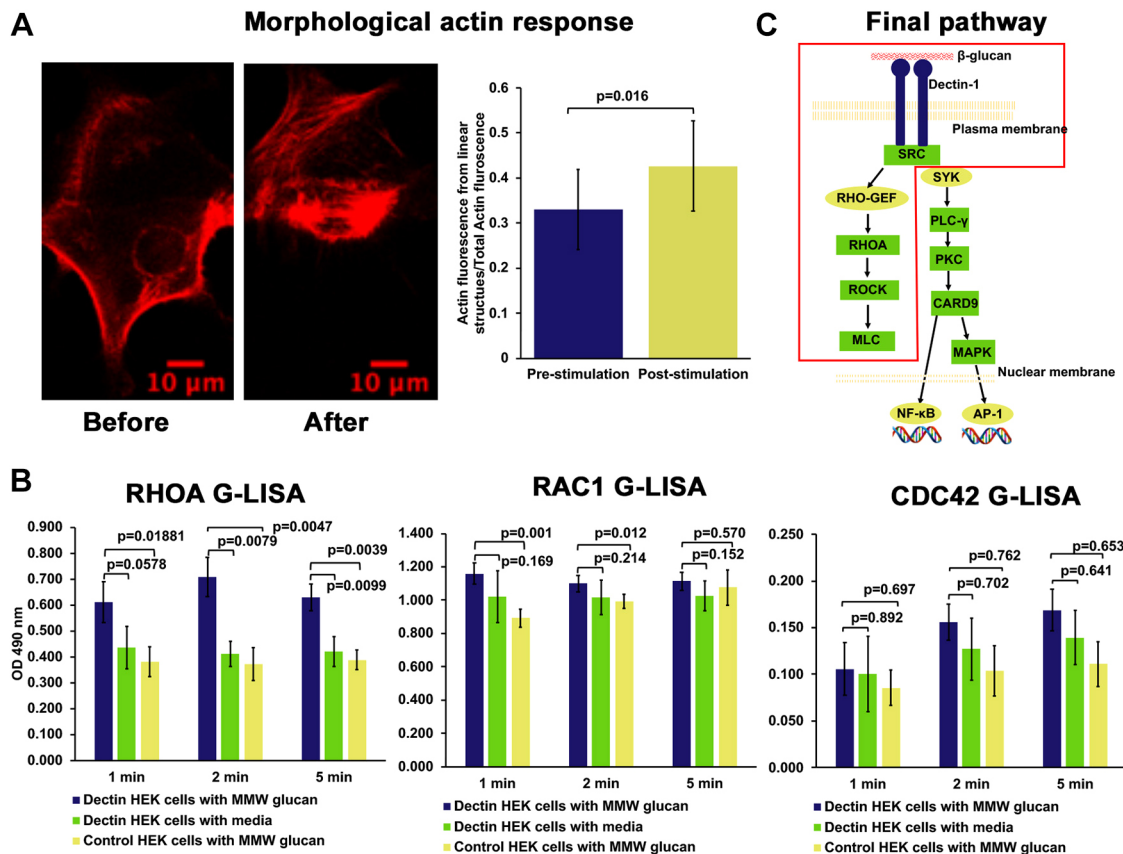


Fig. 3. Activation of RHOA downstream of Dectin-1 after stimulation with glucan. (A) A HEK-293 cell transfected with Emerald-Dectin-1 and mCardinal-LifeAct showing increased actin stress fiber formation 5 min after stimulation with MMW glucan. Graph represents average proportion of actin in linear form as mean \pm s.d. before and 5 min after stimulation with MMW glucan ($n=13$ cells, each from an independent experiment). (B) RHOA, RAC-1 and CDC-42 G-LISA showing significant activation of RHOA after stimulation of Dectin-1-transfected HEK-293 cells with MMW glucan compared to mock stimulation or control HEK-293 cells stimulated with MMW glucan. Bars represent mean \pm s.d. optical density (OD) for each condition for three independent experimental replicates, which were each conducted in triplicate technical replication for each experimental condition. (C) Final schematic of force generation pathway downstream of Dectin-1.

phagocytosis, we used DIC images of HEK-293 cells phagocytosing TRL035 *C. albicans* (Fig. 4D). We predominately found sinking type phagocytosis showing inward pull of fungus, without the presence of prominent pseudopodial engulfment, which is indicative of type II phagocytosis.

DISCUSSION

Dectin-1 engages both SYK-dependent and -independent signaling pathways, and prior literature suggests some context-dependent variability in the signaling mechanisms engaged by this important anti-fungal receptor. Dectin-1-mediated activation of NF- κ B in a SYK-dependent manner, leading to formation of ROS and other immune responses is very well documented (Plato et al., 2013). In contrast, Gringhuis et al. (2009) showed that Dectin-1 also induces a SYK-independent activation of NF- κ B through RAF-1 to control adaptive immune responses. In similar fashion, as mentioned by Goodridge et al. (2012), literature about signaling downstream of Dectin-1 giving rise to phagocytosis is also variable. Even though Dectin-1 signaling clearly leads to activation of SYK, it does not appear to be important in phagocytosis as indicated by our data presented here. Herre et al. (2004) similarly found that phagocytosis downstream of Dectin-1 is SYK independent. We also found that mechanical force generation required for phagocytosis downstream of Dectin-1 is SYK independent. Our data suggest that the Dectin-1-dependent force generation pathway of phagocytosis is mediated

through SFK-dependent activation of an as-yet-unknown RHO-GEF leading to activation of RHOA and ROCK, ultimately leading to the formation and contraction of an actomyosin network. RHOA-mediated contractility during Dectin-1 activation allows the application of tractions on the order of 22.75 pN/ μ m² by the cell on its environment.

We found RHOA plays a very important role in Dectin-1-mediated force generation through actomyosin network formation and contraction in phagocytosis of *C. albicans*. In contrast, Herre et al. (2004) found that CDC42 and RAC1, but not RHOA, play a significant role in phagocytosis downstream of Dectin-1. Their system was different than ours as they used murine NIH/3T3 fibroblast cell line with zymosan particles whereas we used human cell line models and primary human macrophages with a *C. albicans* clinical isolate strain. Therefore, this discrepancy may be explained by Herre et al.'s use of murine cell background and use of particles with much higher level of glucan exposure.

During phagocytosis of apoptotic cells, Tosello-Tramont et al. (2003) and Nakaya et al. (2006) found that RHOA and ROCK have an inhibitory effect on phagocytosis. They found that CDC42 plays a role in phagocytosis of apoptotic cells, and this suggests that CDC42-based type I phagocytosis might be involved in phagocytosis of apoptotic cells compared to involvement of RHOA and ROCK in type II phagocytosis (Olazabal et al., 2002). In Dectin-1-based phagocytosis of *C. albicans*, we think type II sinking phagocytosis is

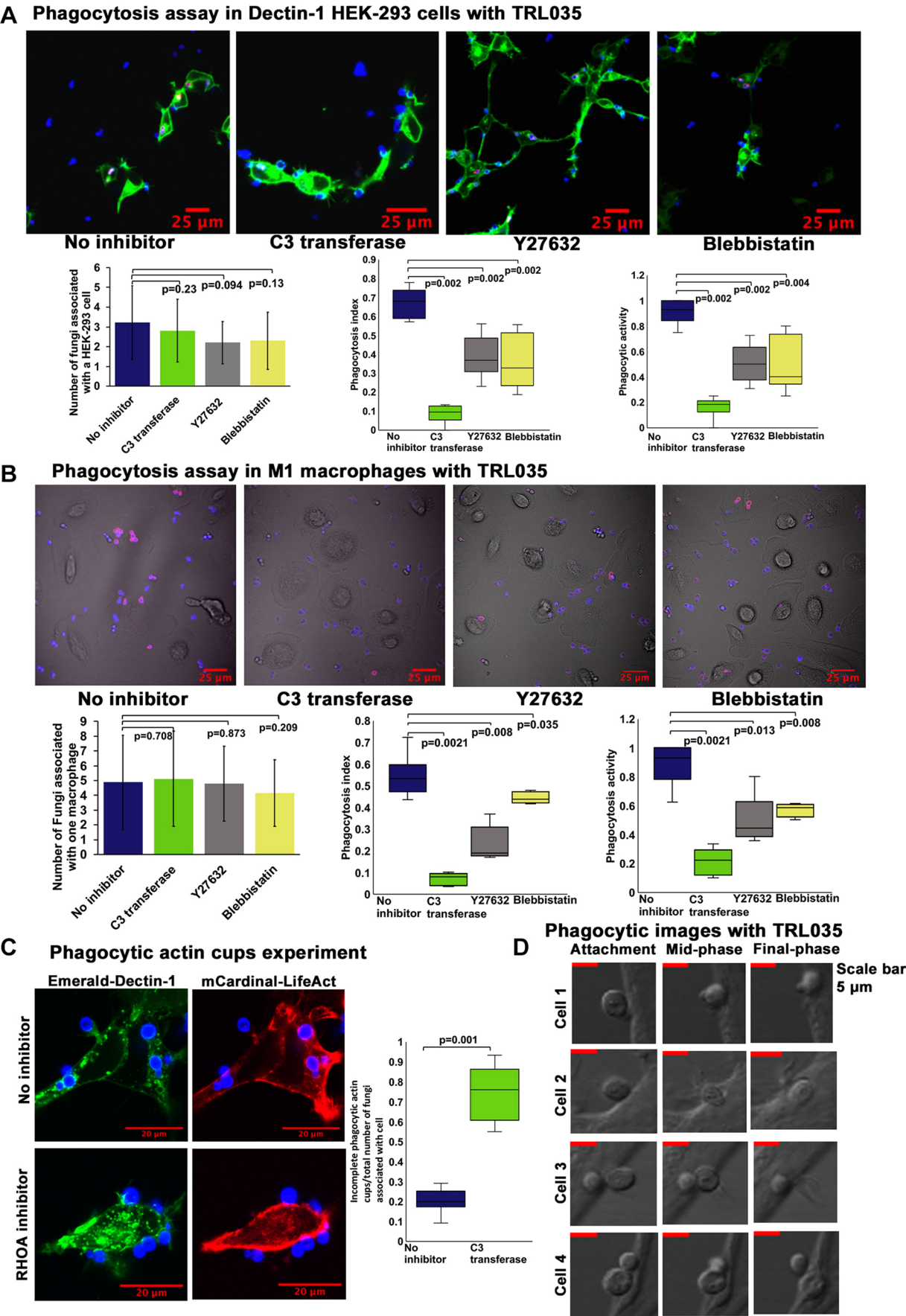


Fig. 4. See next page for legend.

Fig. 4. Relevance of force generation pathway in non-opsonic phagocytosis mediated by Dectin-1.

(A) Phagocytosis assay with HEK-293 cells transfected with Emerald-Dectin-1 and presented with TRL035 *Candida albicans*. *C. albicans* were stained with Calcofluor White (blue) and Cypher5E (red). Images were taken 1 h after introduction of *C. albicans* to culture dishes. HEK-293 cells were either under no inhibitor condition ($n=68$) or pretreated with C3 transferase at 1.5 $\mu\text{g/ml}$ ($n=38$) for 2 h, or Blebbistatin at 12.5 μM ($n=43$) or Y-27632 at 5 μM ($n=69$) for 1 h. Graphs show the mean \pm s.d. number of fungi associated with a single cell, and the phagocytosis index and phagocytic activity under each condition as box plots. (B) Phagocytosis assay in M1 macrophages with TRL035 *C. albicans* under no inhibitor conditions ($n=52$) and with C3 transferase at 1.5 $\mu\text{g/ml}$ ($n=59$), Y-27632 at 5 μM ($n=51$) and Blebbistatin at 12.5 μM ($n=55$). (C) Phagocytosis assay in HEK-293 cells transfected with Emerald-Dectin-1 and mCardinal-LifeAct with TRL035 *C. albicans*. Number of fungi associated with incomplete phagocytic actin cups compared to total number of fungi associated with cell, under no inhibitor ($n=44$) and C3 transferase 1.5 $\mu\text{g/ml}$ ($n=49$) conditions were counted and are shown in the graphs. For the box plots in A,B, the box represents the 25–75th percentiles, and the median is indicated. The whiskers show the minima and maxima. For A–C, the reported value of 'n' denotes the number of total cells pooled from ≥ 3 independent experimental replicates. (D) DIC images of HEK cells transfected with Dectin-1 with TRL035 *C. albicans* showing predominately sinking type II phagocytosis without obvious pseudopodial extensions.

predominantly involved. In sinking phagocytosis, RHOA plays important role in actomyosin network formation. In support of our hypothesis, Colucci-Guyon et al. (2005) and Wiedemann et al. (2006) showed that localized actin assembly, which acts as the driving force for particle engulfment in CR3-mediated type-II phagocytosis is mediated by RHOA. In this study, we consistently observed cell morphologies during phagocytic interaction with yeasts, and cells lacked prominent pseudopodial extensions and exhibited an apparent sinking of the particle in the cell body. Further studies will continue to clarify differential use of phagocytic mechanisms and dependence upon various small GTPases for a variety of relevant cell types, particles and phagocytic routes.

It is possible that the route of phagocytosis may have functional significance. One explanation for why different phagocytosis machinery is used in type I versus type II phagocytosis could be differences in final desired result of phagocytosis: microbicidal versus antigen acquisition. Erwig et al. (2006) found that macrophages engulfing apoptotic cells engaged a rapid, RHOA-dependent process of phagosomal acidification that was much faster than the rate of phagosomal acidification in macrophages engulfing Ig-opsonized particles or DCs engulfing either type of particle. The authors proposed a differential role of RHOA in phagosome maturation depending upon whether the cell type involved was specialized for degradation/eradication versus antigen acquisition from the ingested particles.

Our hypothesis also contrasts with the paper by Kim et al. (2017) wherein ROCK inhibition increased phagocytosis of apoptotic cells, suggesting an initial inhibitory effect of RHOA on phagocytosis in their system. This was later followed by transient RHOA activation prior to closure of phagocytic cup. Transient RHOA activation prior to closure of phagocytic cup was hypothesized by them as an important regulatory step in the 'don't eat me' signaling pathway. Our findings suggest that RHOA may be similarly important for phagocytic cup closure in the Dectin-1 system. Future studies will be necessary to determine whether RHOA activation is also important for earlier stages of Dectin-1-dependent engulfment of fungal pathogens. In terms of mechanics of phagocytosis as mentioned by Herant et al. (2006), the final phase of phagocytosis should involve a 'pull in' force, probably mediated by myosin II. In our study we found Dectin-1-based

phagocytosis of yeast involves mechanical force generation through RHOA and myosin II. This mechanical force should provide the required pull in force for phagocytosis in this final phase.

One more factor which could be driving differential regulation and involvement of the actomyosin machinery in phagocytosis could be particle size. As mentioned by Clarke et al. (2010) and Schlamm et al. (2015), the size of the engulfed particle plays a role in actomyosin responses. In the case of large particles ($>10 \mu\text{m}$), protrusive responses could play a more important role whereas in smaller particles ($<5 \mu\text{m}$), inward pulling force could play a more important role. Overall, it appears that RHO family small GTPases play differential roles in the process of phagocytosis depending on type of phagocytosis, size of particle being phagocytosed and ultimate desired result of phagocytosis.

MATERIALS AND METHODS

Cell culture

HEK-293 cells (ATCC, #CRL-1573) were cultured in DMEM containing 10% FBS, 1% penicillin-streptomycin, 2 mM L-glutamine and 1 mM sodium pyruvate at 37°C, in a 5% CO₂ environment in an incubator. This identity and mycoplasma-free status of the cell line was independently confirmed by submission to ATCC Human Cell Line authentication (STR) and mycoplasma detection (PCR) services.

Transfection

Emerald-Dectin1A-N-10 (Addgene plasmid, #56291; deposited by Michael Davidson). Transfection with Emerald-Dectin-1A-N-10 was performed using standard protocols of Fugene 6 (Promega, #E2691). Cells were selected using Geneticin (G418 sulfate) (Thermo Fisher Scientific, 10131035) at 400 $\mu\text{g/ml}$ for 2 weeks.

M1 macrophages

De-identified primary peripheral blood mononuclear cells (PBMCs) (ATCC, #PCS-800-011) were thawed and cultured using Roswell Park Memorial Institute (RPMI) 1640 medium containing 10% FBS, 1% penicillin-streptomycin, 2 mM L-glutamine and 1 mM sodium pyruvate medium at 37°C, in a 5% CO₂ environment in incubator (Jin and Kruth, 2016). For generation of M1 macrophages, 50 ng/ml rhGM-CSF (PeproTech, #300-03) was added to a culture dish for 7 days followed by stimulation with 500 ng/ml lipopolysaccharide (LPS; Invivogen, #tlrl-pkpls) for 24 h (Fischer et al., 2017; Jin and Kruth, 2016).

MMW glucan

β -1,3;1,6-glucan from *S. cerevisiae* cell wall extraction (~150 kDa) was a generous gift from ImmunoResearch Inc. (Eagan, MN). Glucan was weighed and resuspended in cell culture medium to create a concentrated stock of 1 mg/ml. This concentrated stock was added to the culture vessel on the microscope stage at a 1:10 dilution, which optimized speed of delivery and mixing within the vessel to achieve the stated final glucan concentration.

Contractility assay

HEK-293 cells or M1 macrophages were grown in adherent culture within 35 mm glass bottom Mattek dishes in the absence of any pretreatment of the glass. Cells were stained with CellMask Deep Red Plasma Membrane stain (CMDR) (Invitrogen, #C10046). Stock CMDR from Invitrogen was further diluted to 1:100 in HEK cell medium. This 1:100 diluted CMDR was added to a culture dish at 10 $\mu\text{l/ml}$ of medium in dish for 1 h. Cells were then stimulated with MMW glucan at 8 $\mu\text{g/ml}$ and imaged with a FV1000 laser-scanning confocal microscope (Olympus, Center Valley, PA) with controlled temperature, 37°C, 5% CO₂ for 10 min. A 10 \times lens, 0.40 NA, Plan-Apochromat objective lens was used for imaging. Emerald-Dectin-1 was excited with a 20 mW, 473 nm diode laser operated at 1% power and CMDR was excited with a 20 mW, 635 nm diode laser operated at 2% power. These lines were reflected to the specimen by a 405/473/559/635 multi-edge main dichroic element, routed through a confocal pinhole (110 μm diameter) to dichroics followed by bandpass emission filters in

front of two independent high-sensitivity GaAsP PMT detectors (HSD). Specifically, the emission light passed by the main dichroic was directed to HSD1 (the Emerald–Dectin-1 channel) via a SDM560 filter cube and passage through a BA490–540 nm bandpass filter. For the CMDR channel, a SDM560 filter cube and BA575–675 nm bandpass filter were used. Different conditions used were either no inhibitor condition or pretreatment with various inhibitors for 1 h; BAY-61-3606 (EMD Millipore, #574714) at 500 nM (Yamamoto, 2003), Go6983 (Cayman Chemical Company, #13311) at 2 μ M (Gafni et al., 2013), PD98059 (InvivoGen, #tlrl-pd98) at 12.5 μ M (Alessi et al., 1995), PP1 (Cayman Chemical, #4244) at 10 μ M (Tatton et al., 2003), ML7 (Sigma-Aldrich, #I2764) at 25 μ M (Saitoh et al., 1987), BAPTA-AM (Cayman Chemical, #15551) at 5 μ M (Tang et al., 2007), KN-62 (Cayman Chemical, #13318) at 20 μ M (Tokumitsu et al., 1990), and blebbistatin (Sigma-Aldrich, #203390) at 12.5 μ M, Y-27632 (Sigma-Aldrich, #Y0503) at 5 μ M (Huch et al., 2013). For RHO inhibitor conditions, cells were treated with C3 transferase (Cytoskeleton Inc., #CT04) 1.5 μ g/ml for 2 h. Each experiment was independently replicated at least three times. *n* values and their meanings are detailed in the relevant figure legends.

For quantification of data, to consider effect of inhibitor treatment itself on cell area, we determined the average cell area normalized to that in the untreated control condition. For this, all inhibitor conditions were normalized to a mean cell area of 557.7 μ m² for HEK cells and 1630.2 μ m² for M1 macrophages.

Traction force microscopy

TFM gels were prepared in a similar to that described in Valon et al. (2017). Briefly, the polymerization mixture was placed in a glass-bottom dish and covered with 18 mm round coverslip and left to polymerize for 1 h. Then, the substrates were kept overnight in PBS in 4°C to wash out any potentially non-polymerized acrylamide monomers from the substrate. The next day, the substrates were activated using Sulfo-SANPAH, covered with extracellular matrix (ECM) proteins and incubated for 20 h in 4°C. Afterwards, dishes with substrates were washed three times with PBS and the cells were seeded on substrates.

The first step of TFM experiments was substrate optimization. To find the optimal elasticity and suitable ECM protein cover, substrates of three different elasticities (1 kPa, 8.4 kPa and 19 kPa), similar to ones defined in Tse and Engler (2010), and two ECM proteins (fibronectin and type I collagen), were tested. The aim of this optimization was to find substrates that are soft enough to observe significant cell tractions, but stiff enough to keep cells spread on the substrate. Cells were observed after 3, 6 and 24 h after seeding. After 3 and 6 h, cells were spread on all mentioned substrates; however, after 24 h, cells plated on fibronectin-coated substrates were mostly detached from the substrate, while cells seeded on collagen-coated substrates were still attached to the substrate. Cells grown on collagen-coated substrates of elasticities 19 and 8.4 kPa were well spread, while those on soft substrate (1 kPa) were poorly spread, which suggested they were not strongly attached to the substrate and would be unsuitable for observation of traction forces. This optimization led us to the conclusion that optimal substrate to be used in our TFM experiments was 8.4 kPa coated with type-I collagen.

TFM experiments were performed 18 h after cell seeding, using Zeiss Axio Observer Z1 inverted epifluorescence microscope. In each experiment, four fields of view were observed every 20 s. The aperture of fluorescent light was constrained only to the observed field of view so as to minimize possible cytotoxic effects while illuminating the whole sample with light for a longer time. The continuous TFM experiments were performed for 25 min with an interval of 20 s. At 10 min after the start of the experiment, the solution of MMW glucan was added to reach the final concentration of 8 μ g/ml in cell medium and the responses of the cells were observed for the next 15 min. Analysis of TFM experiments was performed using software provided by X. Trepas, Institute for Bioengineering of Catalonia, Barcelona, Spain (Valon et al., 2017).

To analyze traction forces generated following glucan stimulation, we took an approach that analyzed the typical force fluctuation seen pre-stimulation and compared that to the maximum amplitude of traction force generated shortly after stimulation. We sought to demonstrate that the increases in traction force seen post-stimulation were significantly larger

than the amplitudes of force fluctuation expected from cells that were merely cycling adhesions and migrating upon the surface in the absence of stimulation. For each cell, we calculated the average traction force in the pre-stimulation phase, denoted $\text{mean}(f_{\text{pre}})$. To characterize the force fluctuations in pre-stimulation phase cells, for each independent cell dataset, we calculated the maximum increase (max^+) in traction force relative to the $\text{mean}(f_{\text{pre}})$, denoted $\text{max}^+(\Delta f_{\text{pre}})$:

$$\text{max}^+(\Delta f_{\text{pre}}) = \text{max}(f_{\text{pre}}) - \text{mean}(f_{\text{pre}}).$$

The mean value of $\text{max}^+(\Delta f_{\text{pre}})$ across all measured cells is reported in Fig. 1E. For each individual dataset, the maximum increase in force post-stimulation was measured as $\text{max}^+(\Delta f_{\text{post}})$, the difference between maximum traction force achieved post-stimulation and $\text{mean}(f_{\text{pre}})$:

$$\text{max}^+(\Delta f_{\text{post}}) = \text{max}(f_{\text{post}}) - \text{mean}(f_{\text{pre}}).$$

The mean value of $\text{max}^+(\Delta f_{\text{post}})$ across all measured cells is reported in Fig. 1E. These values from pre- and post-stimulation were compared by Wilcoxon matched-pairs signed rank test to assess probability that post-stimulation response could be explained by the basal (pre-stimulation) force fluctuations observed. These key values for TFM measurements are schematically summarized in Fig. S1.

A total of 25 independent TFM measurements were performed. Twenty of these *n*=25 measurements were used to report TFM results. Five of these datasets were excluded because the data they contained was uninterpretable due to problems arising during the course of data acquisition. In two of the five excluded cases, collapse of cell processes due to cell migration in the pre-stimulation phase caused abrupt changes in traction force that made the baseline traction force unstable and unreliable. In another two of the five excluded cases, floating debris crossing the field during the experiment mechanically interfered with the cells being measured and contaminated traction force results. In the final excluded case, the cell being measured appeared to lose viability during the experiment.

Actin-stress fiber imaging

HEK-293 cells stably expressing Emerald–Dectin-1 were co-transfected with mCardinal–LifeAct-7 using Eugene 6 (Promega#E2691) protocol. mCardinal–Lifeact-7 was Addgene plasmid #54663, deposited by gift from Michael Davidson. Cells were stimulated with glucan at 8 μ g/ml and imaged in Olympus FV1000 confocal system (optical description as for the contractility assay except for using a 60 \times super-corrected, 1.40 NA, Plan-Apochromat oil immersion objective) with a controlled temperature at 37°C and 5% CO₂ for 10 min. Actin stress fibers were quantified using the FSegment MATLAB script developed by Rogge et al. (2017). This script uses a trace algorithm to trace linear structures in image and suppress non-linear fluorescence. Segmented linear structures are then analyzed with respect to fluorescence values for thick and thin actin fibers. Finally, the proportion of fluorescence coming from linear structures compared to total actin fluorescence is calculated. We quantified the proportion of actin in linear form before stimulation and 5 min after stimulation.

G-LISA

The G-LISA activation assay kit RHOA (Cat. #BK124), RAC1 (Cat. #BK128) and CDC42 (Cat. #BK127) from Cytoskeleton, Inc. was used according to manufacturer instructions to measure active GTPase. Dectin-1-transfected HEK-293 cells stimulated with 8 μ g/ml MMW glucan were analyzed for RHOA, RAC1 or CDC42 activation at 1 min, 2 min and 5 min. Control conditions were Dectin-1-transfected cells stimulated with medium (vehicle) and control HEK-293 cells stimulated with MMW glucan. Each experiment was conducted in three independent repeats and results are presented as mean \pm s.d., as described in the figure legend.

Fungal culture

Clinical isolate of TRL035 *C. albicans* was obtained as previously described (Pappas et al., 2016). Isolate was stored as single-use glycerol stock aliquots –80°C. This stock was transferred to 5 ml filter-sterilized yeast extract-peptone-dextrose (YPD) medium (Becton Dickinson) and grown for 16 h at 30°C, with a shaking speed of 300 rpm. The glycerol stock

contained 4×10^7 yeast/ml and was previously calibrated to provide yeast cells at the late log phase under the stated growth conditions (King et al., 1980).

Phagocytosis assay

TRL035 *C. albicans* were first stained with Fluorescent Brightener 28 (Calcofluor White) (Sigma-Aldrich #F3543). 25 μ l of 1 mg/ml Calcofluor White was used to stain 1 ml of 16 h fungal culture in PBS (Gibco) pH 7.4 for 15 min. Then cells were washed three times with PBS and stained with 75 μ M CypHer5E NHS ester (GE Healthcare, PA #15401) for 1 h at 25°C (Pappas et al., 2016). *C. albicans* were then added to culture dishes and observed under a microscope for increased fluorescence in CypHer5E channel as an indicator of fungi that had been phagocytosed. Images were taken with a FV1000 laser scanning confocal microscope (Olympus, Center Valley, PA) equipped with a 60 \times super-corrected, 1.40 NA, Plan-Apochromat oil immersion objective. Calcofluor White (a marker for all yeast) was excited with a 50 mW, 405 nm diode laser operated at 1% power, and Cypher5E was excited with a 20 mW, 635 nm diode laser operated at 0.5% power. These lines were reflected to the specimen by a 405/473/559/635 multi-edge main dichroic element and routed through a confocal pinhole (110 mm diameter) to secondary dichroics followed by bandpass emission filters in front of two independent PMT detectors. Specifically, the emission light passed by the main dichroic was directed to PMT1 (Calcofluor White channel) via reflection from the SDM473 dichroic and passage through a BA430-455 nm bandpass filter. For the Cypher5E channel (HSD detector), light from SDM473 was directed to a SDM560 filter cube and BA575-675 nm bandpass filter. The phagocytosis index and phagocytic activity were calculated using formulae below. Various inhibitor conditions used were the same as in contractility assays (see above).

$$\text{Phagocytosis index} = \frac{\text{Number of fungi phagocytosed by a cell}}{\text{Total number of fungi associated with cell}}$$

$$\text{Phagocytic activity} = \frac{\text{Number of cells which phagocytosed at least one fungus}}{\text{Total number of cells with at least one fungus associated}}$$

Phagocytosis time-lapse imaging

HEK-293 cells transfected with Emerald-Dectin-1 were exposed to TRL035 *C. albicans* in Mattek 35 mm glass-bottom dishes. DIC images were taken with a 60 \times super-corrected, 1.40 NA, Plan-Apochromat oil immersion objective using FV-1000 microscope with 473 nm laser. Cells were imaged for 1 h.

Statistical analysis

Statistical comparisons between samples were carried out using an unpaired two-tailed *t*-test for independent samples. A Wilcoxon matched-pairs signed rank test were used for assessing changes in traction force pre- and post-stimulation. The standard deviation for each sample and *P*-value for comparisons are indicated in figures. For phagocytosis index, phagocytosis activity and actin phagocytic cup index comparison, a Mann-Whitney *U*-test was used. Statistical analyses and graphing were performed with Microsoft Excel 2019 or MATLAB 2018.

Acknowledgements

We gratefully acknowledge technical advice and critical reading of the manuscript by Akram Etemadi Amin, Eduardo Anaya, Carmen Martinez and Matthew Graus. Glucans used in this study were a generous gift from ImmunoResearch Inc, MN., who had no input into experimental design, data interpretation or decision to publish. We thank Xavier Trepas and Carlos-Perez Gonzalez for providing training and technical advice with regard to the TFM methodologies used in this work.

Competing interests

The authors declare no competing or financial interests.

Author contributions

Conceptualization: R.P.C., Z.R., A.N.; Methodology: R.P.C., T.K., A.B., Z.R., A.N.; Formal analysis: R.P.C., T.K., Z.R., A.N.; Investigation: R.P.C., T.K., A.B.; Writing - original draft: R.P.C., T.K.; Writing - review & editing: R.P.C., T.K., A.B., Z.R., A.N.; Visualization: R.P.C., T.K., A.B.; Supervision: Z.R., A.N.; Project administration: A.N.; Funding acquisition: A.N.

Funding

This research was supported by the University of New Mexico Center for Spatiotemporal Modeling of Cell Signaling through the National Institutes of Health (STMC; NIH P50GM085273, to A.K.N.) and R01AI116894 (to A.K.N.). Deposited in PMC for release after 12 months.

Supplementary information

Supplementary information available online at <http://jcs.biologists.org/lookup/doi/10.1242/jcs.236166.supplemental>

References

- Aderem, A. and Underhill, D. M. (1999). Mechanisms of phagocytosis in macrophages. *Annu. Rev. Immunol.* **17**, 593-623. doi:10.1146/annurev.immunol.17.1.593
- Alessi, D. R., Cuenda, A., Cohen, P., Dudley, D. T. and Saltiel, A. R. (1995). PD 098059 is a specific inhibitor of the activation of mitogen-activated protein kinase kinase *in Vitro* and *in Vivo*. *J. Biol. Chem.* **270**, 27489-27494. doi:10.1074/jbc.270.46.27489
- Brown, G. D. (2006). Dectin-1: a signalling non-TLR pattern-recognition receptor. *Nat. Rev. Immunol.* **6**, 33-43. doi:10.1038/nri1745
- Brown, G. D., Taylor, P. R., Reid, D. M., Willment, J. A., Williams, D. L., Martinez-Pomares, L., Wong, S. Y. C. and Gordon, S. (2002). Dectin-1 is a major β -glucan receptor on macrophages. *J. Exp. Med.* **196**, 407-412. doi:10.1084/jem.20020470
- Clarke, M., Engel, U., Giorgione, J., Müller-Taubenberger, A., Prassler, J., Veltman, D. and Gerisch, G. (2010). Curvature recognition and force generation in phagocytosis. *BMC Biol.* **8**, 154. doi:10.1186/1741-7007-8-154
- Colucci-Guyon, E., Niedergang, F., Wallar, B. J., Peng, J., Alberts, A. S. and Chavrier, P. (2005). A role for mammalian diaphanous-related formins in complement receptor (CR3)-mediated phagocytosis in macrophages. *Curr. Biol.* **15**, 2007-2012. doi:10.1016/j.cub.2005.09.051
- Erwig, L.-P., McPhillips, K. A., Wynnes, M. W., Ivetic, A., Ridley, A. J. and Henson, P. M. (2006). Differential regulation of phagosome maturation in macrophages and dendritic cells mediated by Rho GTPases and ezrin-radixin-moesin (ERM) proteins. *Proc. Natl. Acad. Sci. USA* **103**, 12825-12830. doi:10.1073/pnas.0605331103
- Fischer, M., Müller, J. P., Spies-Weissart, B., Gräfe, C., Kurzar, O., Hünig, K., Hochhaus, A., Scholl, S. and Schnetzke, U. (2017). Isoform localization of Dectin-1 regulates the signaling quality of anti-fungal immunity. *Eur. J. Immunol.* **47**, 848-859. doi:10.1002/eji.201646849
- Flannagan, R. S., Jaumouillé, V. and Grinstein, S. (2012). The cell biology of phagocytosis. *Annu. Rev. Pathol. Mech. Dis.* **7**, 61-98. doi:10.1146/annurev-pathol-011811-132445
- Fukata, Y., Kaibuchi, K., Amano, M. and Kaibuchi, K. (2001). Rho-Rho-kinase pathway in smooth muscle contraction and cytoskeletal reorganization of non-muscle cells. *Trends Pharmacol. Sci.* **22**, 32-39. doi:10.1016/S0165-6147(00)01596-0
- Gafni, O., Weinberger, L., Mansour, A. A. F., Manor, Y. S., Chomsky, E., Ben-Yosef, D., Kalma, Y., Viukov, S., Maza, I., Zviran, A. et al. (2013). Derivation of novel human ground state naive pluripotent stem cells. *Nature* **504**, 282-286. doi:10.1038/nature12745
- Goodridge, H. S., Reyes, C. N., Becker, C. A., Katsumoto, T. R., Ma, J., Wolf, A. J., Bose, N., Chan, A. S. H., Magee, A. S., Danielson, M. E. et al. (2011). Activation of the innate immune receptor Dectin-1 upon formation of a 'phagocytic synapse'. *Nature* **472**, 471-475. doi:10.1038/nature10071
- Goodridge, H. S., Simmons, R. M. and Underhill, D. M. (2007). Dectin-1 stimulation by candida albicans yeast or zymosan triggers NFAT activation in macrophages and dendritic cells. *J. Immunol.* **178**, 3107-3115. doi:10.4049/jimmunol.178.5.3107
- Goodridge, H. S., Underhill, D. M. and Toret, N. (2012). Mechanisms of Fc receptor and dectin-1 activation for phagocytosis: mechanisms of fc receptor and dectin-1 activation for phagocytosis. *Traffic* **13**, 1062-1071. doi:10.1111/j.1600-0854.2012.01382.x
- Goodridge, H. S., Wolf, A. J. and Underhill, D. M. (2009). β -glucan recognition by the innate immune system. *Immunol. Rev.* **230**, 38-50. doi:10.1111/j.1600-065X.2009.00793.x
- Gow, N. A. R., van de Veerdonk, F. L., Brown, A. J. P. and Netea, M. G. (2012). Candida albicans morphogenesis and host defence: discriminating invasion from colonization. *Nat. Rev. Microbiol.* **10**, 112-122. doi:10.1038/nrmicro2711
- Gringhuis, S. I., den Dunnen, J., Litjens, M., van der Vliet, M., Wevers, B., Bruijns, S. C. M. and Geijtenbeek, T. B. H. (2009). Dectin-1 directs T helper cell differentiation by controlling noncanonical NF- κ B activation through Raf-1 and Syk. *Nat. Immunol.* **10**, 203-213. doi:10.1038/ni.1692
- Herant, M., Heinrich, V. and Dembo, M. (2006). Mechanics of neutrophil phagocytosis: experiments and quantitative models. *J. Cell Sci.* **119**, 1903-1913. doi:10.1242/jcs.02876
- Herre, J., Marshall, A. S., Caron, E., Edwards, A. D., Williams, D. L., Schweighoffer, E., Tybulewicz, V., Reis E Sousa, C., Gordon, S. and Brown, G. D. (2004). Dectin-1 uses novel mechanisms for yeast phagocytosis in macrophages. *Blood* **104**, 4038-4045. doi:10.1182/blood-2004-03-1140

- Huch, M., Dorrell, C., Boj, S. F., van Es, J. H., Li, V. S. W., van de Wetering, M., Sato, T., Hamer, K., Sasaki, N., Finegold, M. J. et al. (2013). In vitro expansion of single Lgr5+ liver stem cells induced by Wnt-driven regeneration. *Nature* **494**, 247–250. doi:10.1038/nature11826
- Jin, X. and Kruth, H. S. (2016). Culture of macrophage colony-stimulating factor differentiated human monocyte-derived macrophages. *J. Vis. Exp.* **112**, 54244. doi:10.3791/54244
- Kim, S.-Y., Kim, S., Bae, D. J., Park, S. Y., Lee, G. Y., Park, G. M. and Kim, I. S. (2017). Coordinated balance of Rac1 and RhoA plays key roles in determining phagocytic appetite. *PLoS ONE* **12**, e0174603. doi:10.1371/journal.pone.0174603
- King, R. D., Lee, J. C. and Morris, A. L. (1980). Adherence of *Candida albicans* and other *Candida* species to mucosal epithelial cells. *Infect. Immun.* **27**, 667–674. doi:10.1128/IAI.27.2.667-674.1980
- Kovács, M., Tóth, J., Hetényi, C., Málnási-Csizmadia, A. and Sellers, J. R. (2004). Mechanism of blebbistatin inhibition of myosin II. *J. Biol. Chem.* **279**, 35557–35563. doi:10.1074/jbc.M405319200
- Le Cabec, V., Carréno, S., Moisan, A., Bordier, C. and Maridonneau-Parini, I. (2002). Complement receptor 3 (CD11b/CD18) mediates Type I and Type II phagocytosis during nonopsonic and opsonic phagocytosis, respectively. *J. Immunol.* **169**, 2003–2009. doi:10.4049/jimmunol.169.4.2003
- Li, X., Utomo, A., Cullere, X., Choi, M. M., Milner, D. A., Venkatesh, D., Yun, S.-H. and Mayadas, T. N. (2011). The β -glucan receptor dectin-1 activates the integrin Mac-1 in neutrophils via Vav protein signaling to promote *Candida albicans* clearance. *Cell Host Microbe* **10**, 603–615. doi:10.1016/j.chom.2011.10.009
- Liu, M., Luo, F., Ding, C., Albeituni, S., Hu, X., Ma, Y., Cai, Y., McNally, L., Sanders, M. A., Jain, D. et al. (2015). Dectin-1 activation by a natural product β -glucan converts immunosuppressive macrophages into an M1-like phenotype. *J. Immunol.* **195**, 5055–5065. doi:10.4049/jimmunol.1501158
- Nakaya, M., Tanaka, M., Okabe, Y., Hanayama, R. and Nagata, S. (2006). Opposite effects of rho family GTPases on engulfment of apoptotic cells by macrophages. *J. Biol. Chem.* **281**, 8836–8842. doi:10.1074/jbc.M510972200
- Nobes, C. D. and Hall, A. (1995). Rho, Rac, and Cdc42 GTPases regulate the assembly of multimolecular focal complexes associated with actin stress fibers, lamellipodia, and filopodia. *Cell* **81**, 53–62. doi:10.1016/0092-8674(95)90370-4
- O'Brien, X. M., Heflin, K. E., Lavigne, L. M., Yu, K., Kim, M., Salomon, A. R. and Reichner, J. S. (2012). Lectin site ligation of CR3 induces conformational changes and signaling. *J. Biol. Chem.* **287**, 3337–3348. doi:10.1074/jbc.M111.298307
- Olazabal, I. M., Caron, E., May, R. C., Schilling, K., Knecht, D. A. and Machesky, L. M. (2002). Rho-kinase and myosin-II control phagocytic cup formation during CR, but not Fc γ R, phagocytosis. *Curr. Biol.* **12**, 1413–1418. doi:10.1016/S0960-9822(02)01069-2
- Pappas, H. C., Sylejmani, R., Graus, M. S., Donabedian, P. L., Whitten, D. G. and Neumann, A. K. (2016). Antifungal properties of cationic phenylene ethynyls and their impact on β -glucan exposure. *Antimicrob. Agents Chemother* **60**, 4519–4529. doi:10.1128/AAC.00317-16
- Plato, A., Willment, J. A. and Brown, G. D. (2013). C-type lectin-like receptors of the dectin-1 cluster: ligands and signaling pathways. *Int. Rev. Immunol.* **32**, 134–156. doi:10.3109/08830185.2013.777065
- Rogers, N. C., Slack, E. C., Edwards, A. D., Nolte, M. A., Schulz, O., Schweighoffer, E., Williams, D. L., Gordon, S., Tybulewicz, V. L., Brown, G. D. et al. (2005). Syk-Dependent cytokine induction by dectin-1 reveals a novel pattern recognition pathway for C type lectins. *Immunity* **22**, 507–517. doi:10.1016/j.immuni.2005.03.004
- Rogge, H., Artelt, N., Endlich, N. and Endlich, K. (2017). Automated segmentation and quantification of actin stress fibres undergoing experimentally induced changes. *J. Microsc.* **268**, 129–140. doi:10.1111/jmi.12593
- Saitoh, M., Ishikawa, T., Matsushima, S., Naka, M. and Hidakas, H. (1987). Selective inhibition of catalytic activity of smooth muscle myosin light chain kinase. *J. Biol. Chem.* **262**, 7796–7801.
- Schlam, D., Bagshaw, R. D., Freeman, S. A., Collins, R. F., Pawson, T., Fairn, G. D. and Grinstein, S. (2015). Phosphoinositide 3-kinase enables phagocytosis of large particles by terminating actin assembly through Rac/Cdc42 GTPase-activating proteins. *Nat. Commun.* **6**. doi:10.1038/ncomms9623
- Shah, V. B., Ozment-Skelton, T. R., Williams, D. L. and Keshvara, L. (2009). Vav1 and PI3K are required for phagocytosis of β -glucan and subsequent superoxide generation by microglia. *Mol. Immunol.* **46**, 1845–1853. doi:10.1016/j.molimm.2009.01.014
- Sun, L. and Zhao, Y. (2007). The biological role of dectin-1 in immune response. *Int. Rev. Immunol.* **26**, 349–364. doi:10.1080/08830180701690793
- Tang, Q., Jin, M.-W., Xiang, J.-Z., Dong, M.-Q., Sun, H.-Y., Lau, C.-P. and Li, G.-R. (2007). The membrane permeable calcium chelator BAPTA-AM directly blocks human ether a-go-go-related gene potassium channels stably expressed in HEK 293 cells. *Biochem. Pharmacol.* **74**, 1596–1607. doi:10.1016/j.bcp.2007.07.042
- Tatton, L., Morley, G. M., Chopra, R. and Khwaja, A. (2003). The Src-selective kinase inhibitor PP1 also inhibits kit and Bcr-Abl tyrosine kinases. *J. Biol. Chem.* **278**, 4847–4853. doi:10.1074/jbc.M209321200
- Taylor, P. R., Brown, G. D., Reid, D. M., Willment, J. A., Martinez-Pomares, L., Gordon, S. and Wong, S. Y. C. (2002). The β -glucan receptor, dectin-1, is predominantly expressed on the surface of cells of the monocyte/macrophage and neutrophil lineages. *J. Immunol.* **169**, 3876–3882. doi:10.4049/jimmunol.169.7.3876
- Tokumitsu, H., Chijiwa T, Hagiwara M, Mizutani A, Terasawa M and Hidaka H (1990). KN-62, 1-[N,O-bis(5-isoquinolinesulfonyl)-N-methyl-L-tyrosyl]-4-phenylpiperazine, a specific inhibitor of Ca²⁺/calmodulin-dependent protein kinase II. *J. Biol. Chem.* **265**, 4315–4320. doi:10.1016/s0169-5002(96)80017-1
- Tosello-Trampont, A.-C., Nakada-Tsukui, K. and Ravichandran, K. S. (2003). Engulfment of apoptotic cells is negatively regulated by rho-mediated signaling. *J. Biol. Chem.* **278**, 49911–49919. doi:10.1074/jbc.M306079200
- Tse, J. R. and Engler, A. J. (2010). Preparation of hydrogel substrates with tunable mechanical properties. *Curr. Protoc. Cell Biol.* **47**, 10.16.1–10.16.16. doi:10.1002/0471143030.cb1016s47
- Valon, L., Marín-Llauradó, A., Wyatt, T., Charras, G. and Treppe, X. (2017). Optogenetic control of cellular forces and mechanotransduction. *Nat. Commun.* **8**, 14396. doi:10.1038/ncomms14396
- Wiedemann, A., Patel, J. C., Lim, J., Tsun, A., Van Kooyk, Y. and Caron, E. (2006). Two distinct cytoplasmic regions of the β 2 integrin chain regulate RhoA function during phagocytosis. *J. Cell Biol.* **172**, 1069–1079. doi:10.1083/jcb.200508075
- Wilde, C. and Aktories, K. (2001). The Rho-ADP-ribosylating C3 exoenzyme from *Clostridium botulinum* and related C3-like transferases. *Toxicon* **39**, 1647–1660. doi:10.1016/S0041-0101(01)00152-0
- Willment, J. A., Gordon, S. and Brown, G. D. (2001). Characterization of the human β -glucan receptor and its alternatively spliced isoforms. *J. Biol. Chem.* **276**, 43818–43823. doi:10.1074/jbc.M107715200
- Yamamoto, N., Takeshita, K., Shichijo, M., Kokubo, T., Sato, M., Nakashima, K., Ishimori, M., Nagai, H., Li, Y.-F. and Yura, T. et al. (2003). The orally available spleen tyrosine kinase inhibitor 2-[7-(3,4-Dimethoxyphenyl)-imidazo[1,2-c]pyrimidin-5-ylamino]nicotinamide Dihydrochloride (BAY 61-3606) blocks antigen-induced airway inflammation in rodents. *J. Pharmacol. Exp. Ther.* **306**, 1174–1181. doi:10.1124/jpet.103.052316
- Yi, J., Wu, X. S., Crites, T. and Hammer, J. A. (2012). Actin retrograde flow and actomyosin II arc contraction drive receptor cluster dynamics at the immunological synapse in Jurkat T cells. *Mol. Biol. Cell* **23**, 834–852. doi:10.1091/mbc.e11-08-0731